Final Technical Report for DOE-FG02-07ER15913

Molecular Design of Zinc Oxide Nanocrystal-Dye Dyads and Triads

Project Period Dates: 09/01/2007 to 08/31/2016

Principal Investigator:	Prof. Wayne L. Gladfelter Department of Chemistry University of Minnesota 207 Pleasant St., SE Minneapolis, MN 55455
Co-Principal Investigators:	Prof. Kent R. Mann Department of Chemistry, University of Minnesota Prof. David A. Blank Department of Chemistry, University of Minnesota
Applicant/Institution:	University of Minnesota 450 McNamara Alumni Center 200 Oak St., SE Minneapolis, MN 55455
DOE/Office of Science Program:	Office of Basic Energy Sciences

Contents — Page Number

I. Introduction and Overview 3
II. Final Report 4
A. Nanocrystal platforms and dyes 4
B. Binding and Static Quenching Behavior of a Terthiophene Carboxylate on Monodispersed ZnO Nanocrystals 5
C. Spectroscopic Investigations of Energy and Charge Transfer Dynamics 6
1. Using Quantum Confinement to tune electron transfer rates in Zinc Porphyrin/ZnO Nanocrystal Ethanol Solutions 6
2. Electron Transfer Dynamics of a Terthiophene Carboxylate on Monodispersed Zinc Oxide Nanocrystals 7
3. Internal Charge Transfer in Substituted Terthiophenes 7
D. Secondary Electron Donors 8
E. Phosphonate vs. Carboxylate Anchors 9
III. References 9

I. Introduction and Overview

The overall energy conversion efficiency of solar cells depends on the combined efficiencies of light absorption, charge separation and charge transport.[1,2] The most efficient dye-sensitized solar cells (DSSCs) use nanocrystal TiO_2 films to which are attached ruthenium complexes such as **N3** and **N719.**[1,3] Numerous studies have provided valuable insight into the dynamics of these and analogous photosystems,[2,4] but the lack of site homogeneity in binding dye molecules to TiO_2 films and nanocrystals (NCs) is a significant impediment to extracting details about the electron transfer across the interface.[2,5-7]

Although zinc oxide is emerging as a potential semiconducting component in DSSCs,[8-11] there is less known about the factors controlling charge separation across the dye/ZnO interface. Zinc oxide crystallizes in the wurtzite lattice and has a band gap of 3.37 eV. One of the features that makes ZnO especially attractive is the remarkable ability to control the morphology of the films. Using solution deposition processes, one can prepare NCs, nanorods and nanowires having a variety of shapes and dimensions.[12-22] As an example of this control, Figure 1 includes a TEM of ZnO NCs that were prepared in gram quantities by a nonaqueous process (described in section II.A) in Professor Gladfelter's laboratory.[22]

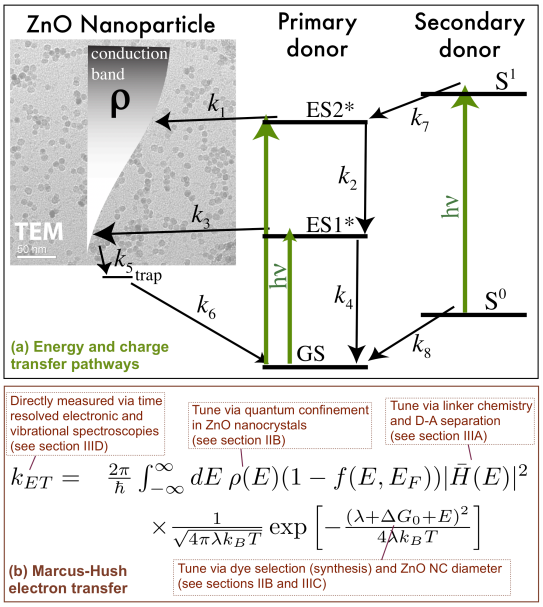

Figure 1 (a) Schematic illustration of some of the dynamics associated with dye sensitized energy and electron transfer. On the left is a TEM image of an example of the ZnO NCs prepared in our laboratory. (b) Marcus theory for electron transfer into a continuum of acceptor states[4] and reference to sections of this proposal outlining systematic probing of the salient components.

This report outlines studies that overcome the problems associated with film heterogeneity through the use of dispersible sensitizer/ZnO NC ensembles. The overarching goal of this research was to study the relationship between structure, energetics and dynamics in a set of synthetically controlled donor-acceptor dyads and triads. These studies provided access to unprecedented understanding of the light absorption and charge transfer steps that lie at the heart of DSSCs, thus enabling significant future advances in cell efficiencies. Our approach began with the construction of well-defined dye-NC dyads that were sufficiently dispersible to allow the use of state of the art pulsed laser spectroscopic and kinetic methods to understand the charge transfer events at a fundamental level. This was combined with the synthesis of a broad range of sensitizers that provide systematic variation of the energetics, excited state dynamics, structure and interfacial bonding. The key was that the monodisperse nature and high dispersibility of the ZnO NCs will made these experiments reproducible; in essence, the measurements were on discrete molecular species rather than on the complicated mixtures that result from the typical fabrication of functional photovoltaic cells. The monodispersed nature of the NCs also allowed the use of quantum confinement to investigate the role of donor/acceptor energetic alignment in chemically identical systems. Our results added significantly to our basic understanding of energy and charge transfer events at molecule-

semiconductor interfaces (Figure 1) and helped the R&D community realize zinc oxide's full potential in solar cell applications.

II. Final Report

We have accomplished the following:

- developed a new approach to multigram quantities monodispersed ZnO nanocrystals,[22,23]
- characterized the photophysics of electronically tuned disubstituted terthiophene complexes,[24]
- measured the binding constant of a terthiophene acid dye on ZnO NCs and established the static quenching behavior,[25]
- measured the charge injection dynamics for a terthiophene acid:NC as a function of coverage,[26]
- demonstrated control of the electron transfer rate by tuning the density of acceptor states in ZnO NC using quantum confinement,[27]
- initiated ultrafast charge injection studies for a broad range of potential dye sensitizers - ZnO NC dyad dispersions,
- synthesized new dyes: 8 Ru complexes, 6 Ir complexes, 2 new porphyrin complexes (Zn, Pd),
- compared the excited state electron transfer rates of terthiophene chromophores bound by a carboxylate anchor to a phosphonate anchor.

II.A. Nanocrystal Platforms and Dyes. Two different nanocrystal syntheses allow studies in polar and nonpolar solvents: a flexibility that accommodates dyes of varying solubility. Most literature approaches generate ZnO NCs using water and/or hydroxide in polar solvents,[14,15,28-30] and these have formed the basis for most of our studies. After synthesizing a number of possible precursors,[23] a route to ZnO NCs dispersible in nonpolar solvents was based on the reaction of an amide precursor, $[Zn(N^iBu_2)_2]_2$, with hexylamine followed by reactions of the as-formed solution in a moist air flow.[22] Room temperature reactions led to monodisperse 2.8-5.3 nm NCs with the sizes increasing in direct proportion to the relative humidity. Purification afforded multigram quantities of stable NCs that were dispersible in nonpolar solvents. In addition to providing H_2O to serve as the

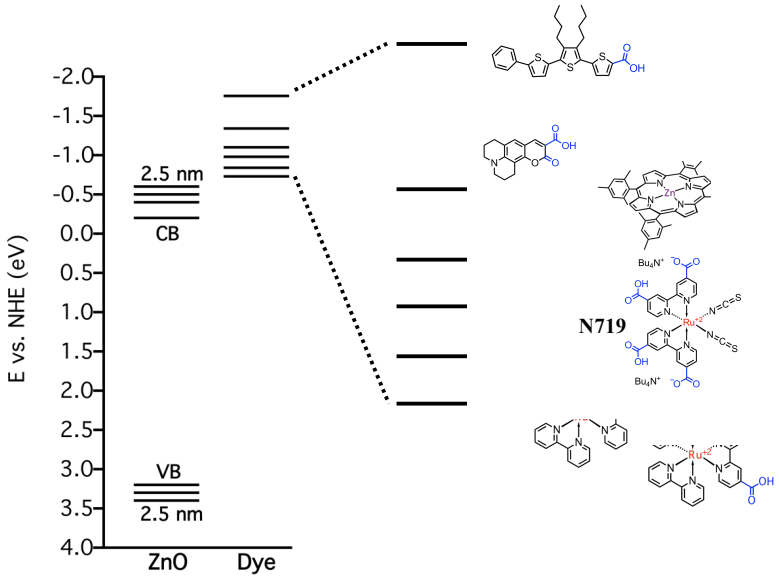

Figure 2. Energy diagram comparing the excited state oxidation potentials of several dyes (right) to the valence and conduction band edges of bulk ZnO and several nanocrystals.

source of oxygen in the ZnO, the airflow adds CO_2 that converts the alkylamine into an alkyl-ammonium alkylcarbamate, which serves as the surfactant and stabilizes dispersions in solvents as nonpolar as hexane.

Figure 2 summarizes the relative energies of ZnO NCs and a selection of dyes studied to date. With the small NCs used in this study, the conduction band edge increases sufficiently that the ET process becomes unfavorable for some dyes. Of the dyes examined, ranging in excited state potentials from -0.73 to -1.3 V (vs. NHE), the ZnO NCs quenched the excited state of four. Neither $[Ru(bpy)_3]^{2+}$ nor $[Ru(bpy)_2(dcbpy)]^{2+}$ the two with the lowest excited state potentials, were quenched. We have found, however, that adding electron donating substituents (diethylamino, pyrrolidino, piperidino and morpholino) to the 4 and 4' position of the two bpy ligands of $[Ru(bpy)_2(dcbpy)]^{2+}$ increases the energy of the excited state to ~ -1 V and leads to fluorescent dyes that are quenched by the ZnO NCs. *Although fluorescence is not a requirement for an effective solar cell dye or even for our ultrafast measurements of energy and charge transfer, the absence of static quenching can exclude charge injection. When combined with studies that demonstrate charge injection as the primary quenching mechanism (for example see section II.C.2), static quenching does provide us with an effective and quantitative method to evaluate the bonding between the NC and the dye.*

In sections IIB-C we describe studies of two dyes, 3',4'-dibutyl-2-phenyl-2,2':5',2"-terthiophene-5"-carboxylic acid, **1-CO_2^-** (Figure 3) and 5-(4-carboxyphenyl)-10,15,20-trimesitylporphyrinatozinc (II), **2** (Figure 4). The comparison is interesting. Unlike the results found for the porphyrin complex (E* = -1.03 V),[27] no measurable effect of NC diameter on k_{ET} was observed for the more energetic excited state of the terthiophene acid (E* = -1.3 V).[26] Based on this experimental result, many of our new dyes are designed to have E* values around -1 V, where we anticipate greater sensitivity to changes in the factors included in the preexponential term of the Marcus equation (Figure 1b).

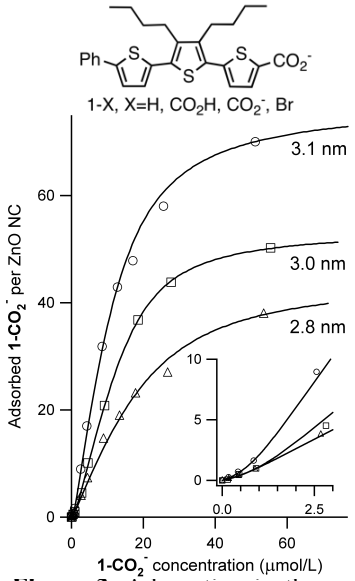

Figure 3. Adsorption isotherms of **1-CO_2H** on ZnO NCs (points) fit with a model that includes the competitive binding of **1-CO_2^-** to both ZnO and Zn^{2+} (solid lines). The inset shows the low concentration regime.

II.B. Binding and Static Quenching Behavior of a Terthiophene Carboxylate on Monodispersed ZnO Nanocrystals. The details of this study have been published.[25] The terthiophene-based dye, **1-CO_2H**, was found to bind to ZnO NCs as the carboxylate and its excited state was quenched. For a constant concentration of NCs, measurement of the proportion of bound vs. unbound **1-CO_2^-** as a function of dye concentration produced an adsorption isotherm that was fit to a Langmuir model. The value of K_{ads} of 2.3 ± 1.0 x 10^5 M^{-1} did not depend on the size of the NC, but the maximum number of adsorbed dyes per NC increased with increasing NC diameter (Figure 3). At low dye concentrations, observation of a small deviation of the experimental values from the Langmuir model was attributed to a second equilibrium in which a portion of the dye was ligated to free zinc ions. Although linear at lower quencher (ZnO NC) concentrations Stern-Volmer plots exhibited complex behavior, which was also consistent with the presence of free zinc ion in the

solutions. An additional test was applied that confirmed the importance of the $-CO_2^-$ binding group. Replacement of the $-CO_2H$ functional group with a -Br resulted in little change to excited state potential and spectroscopic properties of the molecule. Fluorescence measurements, however, established the excited state of **1-Br** was not quenched by the presence of ZnO. *This comparison emphasizes the static nature of the quenching process and the importance of the $-CO_2^-$ binding group for quenching.*

II.C. Spectroscopic Investigations of Energy and Charge Transfer Dynamics. Using time integrated and ultrafast time resolved spectroscopic methods we investigated the energy and charge transfer dynamics in low concentration solutions of the ZnO NCs with both known and new sensitizers. In the case of the standard benchmark system, **N719**, the charge injection at low **N719**:ZnO ratios was determined using transient absorbance to be single exponential with a time constant of 29 ps. This was in contrast with the results reported on nanocrystalline surfaces, where the charge injection was multiphasic and spanned timescales from <1ps to 100's of ps.[2,4,31-36] The difference highlighted the complexity of nanocrystalline film surfaces and demonstrated our ability to investigate the charge transfer under conditions that were better defined. Using ultrafast fluorescence methods we measured the charge transfer rates from Coumarin 343 and the zinc porphyrin (**2** - see Figure 4) to ZnO NCs. In both cases the injection dynamics were single exponential. Our measured time constant of 2.3 ps for Coumarin 343 was similar to the earlier report of Castner and coworkers,[37] however we did not see evidence for the additional 330 fs injection component, which they reported. In the case of the zinc porphyrin, the time constant we measured was roughly 300 ps, and it depended on the average size of the ZnO particles. This intriguing result is discussed in more detail in the next section.

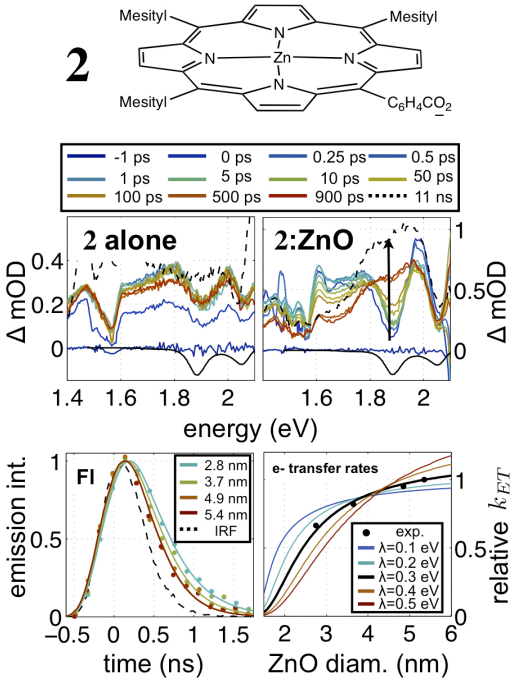

Figure 4: Frequency-resolved pump-probe, time resolved fluorescence measurements of **2** and a **2**/ZnO nanocrystal mixture in EtOH.

II.C.1. Using Quantum Confinement to Tune Electron Transfer Rates in Zinc Porphyrin/ZnO Nanocrystal Ethanol Solutions. The details of this work have been published.[27] We investigated the electron injection rates for a series of size selected ZnO NCs and the tetraphenylporphyrin derivative, **2**, shown in Figure 4. Time-integrated fluorescence experiments confirmed excited state quenching by ZnO. Time-resolved fluorescence and time- and spectrally-resolved pump-probe measurements for an approximately 1:1 mixture of **2** and ZnO NCs are shown in Figure 4. These results confirmed a reduced excited state lifetime for the **2**/ZnO mixtures compared to the free **2** in solution. Directly probing the porphyrin cation radical confirmed the quenching mechanism as charge transfer, see Figure 4.

Charge injection occurred with a time constant of approximately 300 ps, which was slow compared to similar systems on TiO_2.[38] This time constant was found to be sensitive to the size of the NCs as shown in Figure 4, varying from 369 ps for 2.9 nm NCs to 245 ps for 5.9 nm NCs.

Within the typical assumption of diabatic electron transfer (Marcus Theory, see Figure 1b) the ET rate depends on both the free energy barrier in the exponential term and a pre-exponential term that includes the density of acceptor states.[2,4] The free energy barrier can be exploited to exert dramatic influence on the ET rate.[39] However, when there is an energetic distribution of available acceptor states, such as the case for ZnO, the rate can be dominated by barrierless transfer,[4] and thus controlled by the pre-exponential terms. We demonstrated that by shifting the conduction band edge of the ZnO via size selection of the NCs, we could tune the density of accepting states near energetically barrierless electron transfer and directly observe the subsequent influence on the ET rates. To our knowledge this represents the first such demonstration using quantum confinement to influence the ET rates via tuning the density of acceptor states without altering the chemistry of the system in any way.

II.C.2. Electron Transfer Dynamics of a Terthiophene Carboxylate on Monodispersed Zinc Oxide Nanocrystals. The details of this work have been published.[26] Having established that **1-CO$_2^-$** binds to, and its excited state was quenched by ZnO NCs (section II.B), we used a combination of full frequency pump-probe and time resolved fluorescence to investigate the charge transfer between the dye and ZnO NC. The absorption spectrum of the **1-CO$_2^{\bullet}$**, was characterized using spectroelectrochemistry, and transient absorption experiments confirmed the quenching mechanism to be electron transfer. As an example, pump-probe spectra for the terthiophene dye and a 1:1 dispersion of the dye with 3 nm ZnO NCs in ethanol are shown in Figure 5. Transient absorption decay of the initially excited state, time-resolved fluorescence measurements, and measurements of the rise in the transient absorption of the radical, **1-CO$_2^{\bullet}$**, were all consistent, indicating near single exponential electron transfer kinetics with a time constant of 3.5 ps. Measurements were repeated for several mixtures with dye:NC concentration ratios varying from 240:1 to 1:2. As a function of the ratio, the charge injection efficiency mirrored the complex time-integrated emission quenching measurements (section II.B), reaching a maximum at ratios corresponding to roughly monolayer coverage on the NCs (approximately 20 dyes per NC). At dye:NC ratios below the maximum injection efficiency, the relative decrease in charge injection with increasing ZnO concentration was the result of competitive binding, as discussed in section II.B. The lack of concentration quenching at high surface coverage was likely the result of steric interference from the butyl groups minimizing electronic coupling between adjacent dye molecules. The potential to get to high surface coverage without loss of injection efficiency from the bound sensitizer molecules is a significant potential advantage of this class off dyes in the context of DSSCs.

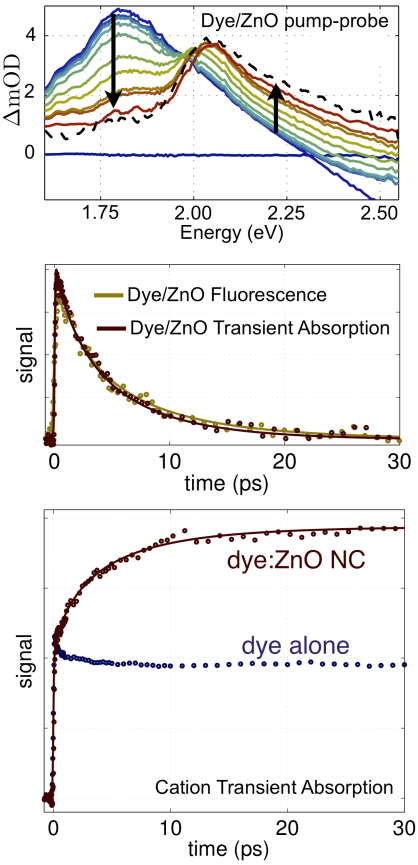

Figure 5: Spectroscopic data for terthiophene dye, **1-CO$_2^-$**, and a ~1:1 **1-CO$_2^-$**/ZnO mixture in ethanol. *Top:* Pump-continuum probe spectra. *Middle:* Comparison of fluorescence upconversion at 2.55 eV and transient absorption at 1.65 eV. *Bottom:* Transient absorption of the cation product at 2.06 eV.

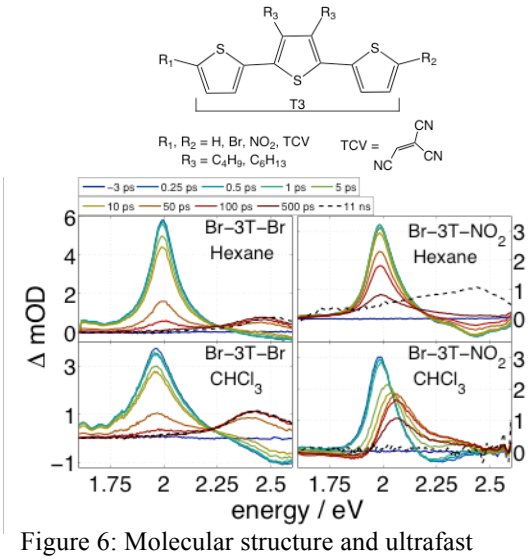

Figure 6: Molecular structure and ultrafast pump-continuum probe spectra for substituted terthiophene derivatives in hexane and chloroform solutions.

II.C.3. Internal Charge Transfer in Substituted Terthiophenes. The details of this work have been published.[24] In order to maximize the usefulness of oligothiophenes in solar cell applications it is advantageous to have the ability to tune their electronic properties via chemical modification. Substitution with electron withdrawing and donating groups is a viable method for this,[40-42] however it can have substantial effects on excited state relaxation dynamics and other spectroscopic properties. By taking advantage of the synthetic capability to vary the substituents systematically we were able to measure the influence of internal charge transfer on excited state lifetime and intersystem crossing (ISC). Using a combination of fluorescence quantum yield, frequency resolved pump-probe spectroscopy, and ultrafast time resolved emission; we measured both internal conversion (IC) and ISC rates. Examples of the pump-probe measurements are shown in Figure 6. ISC and IC rates changed by more than an order of magnitude as the electron withdrawing ability of the substituents was tuned. Increasing the degree of charge separation in the excited state (Figure 7) not only decreased the ISC rate, but also at the same time it tended to increase the IC rates. The effects were substantial. For example, in the asymmetrically substituted molecules we observed *a factor of 20 decrease in the ISC rates going from hexane to toluene* as a result of the stabilization of the excited state. In more polar solvents such as acetone, the IC rate increased by an order of magnitude. This work also demonstrated the same effects in symmetrically substituted molecules, where a first-order estimation might suggest that symmetry would eliminate the charge separated nature of the excited state. However, at finite temperatures in condensed environments the symmetry was lost and the same set of large changes in excited state dynamics were observed for both the symmetric and asymmetric analogues. Overall we found that when using chemical modification to tune the electronic properties of the sensitizers, it was critical to also take into consideration the influence that such modifications can have on the excited state dynamics. The effects were particularly significant in highly polar condensed environments such as those found in DSSCs.

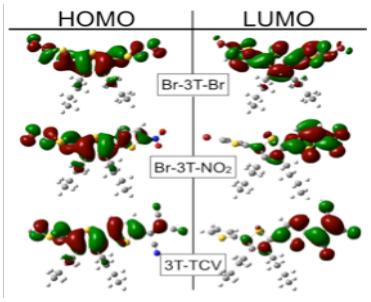

Figure 7: HF-631G(d) optimized structures and molecular orbital diagrams for bromo, nitro, and TCV substituted terthiophene derivatives

II.D. Secondary Electron Donors. In addition to dyads involving ZnO NCs, we explored the behavior of molecular dyads in which the primary chromophore was coupled to a secondary electron donor. Suitably functionalized derivatives of these molecular dyads will be attached to the ZnO NCs in future work. We synthesized and initiated detailed absorption, emission and electrochemical studies of a series of cationic Ir(III) complexes of the type $[Ir(C^N)_2(N^N)]^+$ (C^N = cyclometalating ligand, N^N = diimine ligand) that incorporated cyclometalating ligands

bearing functionalized terthiophenes (3Ts) as secondary electron donors (SEDs) and diimine ligands possessing nitro substituent electron acceptors (EWG) (Figure 8).

Similar to the well-studied Ru(II) polypyridyl complexes, the lowest unoccupied molecular orbital (LUMO) in these cationic Ir(III) cyclometalates resided on the N^N ligand but in contrast, the highest occupied molecular orbital (HOMO) possessed significant ligand character, with electron density on both the phenyl portion of the C^N ligands and the Ir(III) center. The enhanced spatial separation of the HOMO and LUMO on different ligands in these cationic Ir(III) cyclometalates allowed the selective tuning of their electrochemical and spectral properties by proper synthetic modification and led to high directionality and increased spatial separation between the radical ion pair generated upon photoexcitation. The new compounds reported here also addressed the poor photon-to-current efficiency (IPCE) response of the previously studied Ir(III) systems as the secondary electron donors (SEDs) also increased the spectral coverage and molar absorptivities of the complexes.

Introduction of the functionalized 3T-SED pendants to the pyridyl half of the appropriate C^N ligand was accomplished through a Stille coupling of the respective fragments. The site location of the 3T-SED pendants within complexes **3** and **4** was selected to ensure minimal interaction with the electronic ground state of the complexes as demonstrated through minimal perturbation of the Ir(III)/Ir(IV) oxidation couple (occurs at about +1.35 V) after complexation of a (C^N)-3T-SED ligand to an Ir(III) center. Additionally, in cyclic voltammetric studies of 3T-SED complexes **3** and **4,** oxidation of the 3T-SED pendants were found at lower potentials (+1.05 V) with respect to the Ir(III)/(IV) couple. This ordering of redox couples suggests the hole will reside on the 3T-SED pendants after photoexcitation. From preliminary emission data that give an estimated excited state energy of ~ 2.0 V, these results suggest an E* value of around -1.0 V for these complexes. These results nicely set up our studies of the photoinduced charge transport from these dyes to the ZnO NC's by ultrafast spectroscopy.

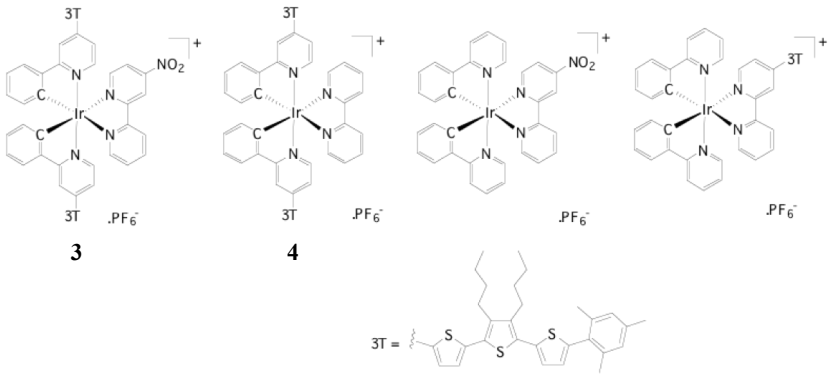

Figure 8. Cyclometallated Ir dyes bearing excellent electon donating (terthiophene) or accepting (nitro) substituents or both.

As the LUMO resides mainly on the diimine ligand within these complexes, this ligand was modified with the powerful electron acceptor (nitro functionalized bpy). Facile reduction of the nitro-bipyridine (-0.5 V compared to bpy at -1.3 V) in 3T-SED complexes **3** and **4** suggests that this portion of the molecule acts as the terminal electron acceptor during the photoinduced charge transfer events. The presence of the nitro substituent on the diimine ligand resulted in a large LUMO stabilization of nearly 0.8 V but virtually no shift in the oxidations of either the Ir or the 3T pendant. Additionally a large decrease in the HOMO-LUMO gap was observed as a red shift in the optical absorption spectra. The synthesis, electrochemistry and spectroelectrochemical results we have collected for these compounds are reported in a manuscript that is nearly ready for submission. This information has been useful for interpreting the ultrafast spectroscopy results we are also in the process of collecting. These time resolved

transient absorption experiments are designed to observe and characterize the resultant radical ion pair due to intraligand photo-induced electron transfer. Synthetic attempts to replace the nitro substituent with carboxy groups for anchoring to ZnO nanocrystals used in DSSC applications are underway.

IIE. Phosphonate vs. Carboxylate Anchors. Terthiophene dyes were synthesized having a carboxylate or phosphonate moiety at the 2-position which serves as an anchoring group to zinc oxide nanocrystals (ZnO NCs). Electronic absorption and fluorescence measurements, combined with reduction potentials, provided estimates of -1.49 and -1.63 V vs. NHE for the excited state reduction potential of the carboxylate and phosphonate, respectively. Static quenching was observed when the dyes were bound to the surface of acetate-capped ZnO NCs having a diameter of 2.8 nm. Stern-Volmer studies conducted at several dye concentrations established that a minor fraction of adsorbed dye remained unquenched even at 1:1 dye to NC ratios. Adsorption isotherm measurements establish that the phosphonate binds more strongly than the carboxylate and that saturation coverage is ~1.2 dyes/nm^2 for both dyes. Ultrafast transient absorption spectroscopic experiments were used to probe the lifetimes of the dyes' excited singlet state. In the presence of ZnO NCs, the disappearance of the singlet excited states of the dyes corresponded to the appearance of the spectroscopic signatures of the oxidized dyes and occurred with lifetimes of 1.5 ± 0.1 and 6.1 ± 0.2 ps, respectively for the carboxylate and phosphonate dye. The difference in the electron transfer rates was attributed to a larger electronic coupling for the dye having the carboxylate anchoring group.

III. References

(1) Graetzel, M. "Solar Energy Conversion by Dye-Sensitized Photovoltaic Cells", *Inorg. Chem.* **2005**, *44*, 6841, doi:

(2) Ardo, S.; Meyer, G. J. "Photodriven heterogeneous charge transfer with transition-metal compounds anchored to TiO2 semiconductor surfaces", *Chem. Soc. Rev.* **2009**, *38*, 115, doi:

(3) O'Regan, B.; Graetzel, M. "A low-cost, high-efficiency solar cell based on dye-sensitized colloidal titanium dioxide films", *Nature* **1991**, *353*, 737, doi:

(4) Anderson, N. A.; Lian, T. "Ultrafast electron transfer at the molecule-semiconductor nanoparticle interface", *Annu. Rev. Phys. Chem.* **2005**, *56*, 491, doi:

(5) Tachibana, Y.; Nazeeruddin, M. K.; Gratzel, M.; Klug, D. R.; Durrant, J. R. "Electron injection kinetics for the nanocrystalline TiO2 films sensitized with the dye (Bu4N)2Ru(dcbpyH)2(NCS)2", *Chemical Physics* **2002**, *285*, 127, doi:

(6) Kallioinen, J.; Benkoe, G.; Myllyperkioe, P.; Khriachtchev, L.; Skrman, B.; Wallenberg, R.; Tuomikoski, M.; Korppi-Tommola, J.; Sundstroem, V.; Yartsev, A. P. "Photoinduced Ultrafast Dynamics of Ru(dcbpy)2(NCS)2-Sensitized Nanocrystalline TiO2 Films: The Influence of Sample Preparation and Experimental Conditions", *J. Phys. Chem. B* **2004**, *108*, 6365, doi:

(7) Wenger, B.; Graetzel, M.; Moser, J.-E. "Rationale for Kinetic Heterogeneity of Ultrafast Light-Induced Electron Transfer from Ru(II) Complex Sensitizers to Nanocrystalline TiO2", *Journal of the American Chemical Society* **2005**, *127*, 12150, doi:

(8) Law, M.; Greene, L. E.; Johnson, J. C.; Saykally, R.; Yang, P. "Nanowire dye-sensitized solar cells", *Nature Materials* **2005**, *4*, 455, doi:
(9) Wolden, C. A.; Barnes, T. M.; Baxter, J. B.; Aydil, E. S. "Infrared detection of hydrogen-generated free carriers in polycrystalline ZnO thin films", *Journal of Applied Physics* **2005**, *97*, 043522/1, doi:
(10) Baxter, J. B.; Aydil, E. S. "Dye-sensitized solar cells based on semiconductor morphologies with ZnO nanowires", *Solar Energy Materials & Solar Cells* **2006**, *90*, 607, doi:
(11) Ravirajan, P.; Peiro, A. M.; Nazeeruddin, M. K.; Graetzel, M.; Bradley, D. D. C.; Durrant, J. R.; Nelson, J. "Hybrid Polymer/Zinc Oxide Photovoltaic Devices with Vertically Oriented ZnO Nanorods and an Amphiphilic Molecular Interface Layer", *J. Phys. Chem. B* **2006**, *110*, 7635, doi:
(12) Bahnemann, D. W.; Kormann, C.; Hoffmann, M. R. "Preparation and characterization of quantum size zinc oxide: a detailed spectroscopic study", *Journal of Physical Chemistry* **1987**, *91*, 3789, doi:
(13) Spanhel, L.; Anderson, M. A. "Semiconductor clusters in the sol-gel process: quantized aggregation, gelation, and crystal growth in concentrated zinc oxide colloids", *Journal of the American Chemical Society* **1991**, *113*, 2826, doi:
(14) Meulenkamp, E. A. "Synthesis and Growth of ZnO Nanoparticles", *J. Phys. Chem. B* **1998**, *102*, 5566, doi:
(15) Wong, E. M.; Bonevich, J. E.; Searson, P. C. "Growth kinetics of nanocrystalline ZnO particles from colloidal suspensions", *J. Phys. Chem. B* **1998**, *102*, 7770, doi:
(16) Schwartz, D. A.; Gamelin, D. R. "A simple room-temperature preparation of colloidal ZnO quantum dots from homogeneous polar aprotic solutions", *Proceedings of SPIE-The International Society for Optical Engineering* **2003**, *5224*, 1, doi:
(17) Law, M.; Goldberger, J.; Yang, P. "Semiconductor nanowires and nanotubes", *Annual Review of Materials Research* **2004**, *34*, 83, doi:
(18) Yin, M.; Gu, Y.; Kuskovsky, I. L.; Andelman, T.; Zhu, Y.; Neumark, G. F.; O'Brien, S. "Zinc Oxide Quantum Rods", *J. Am. Chem. Soc.* **2004**, *126*, 6206, doi: 10.1021/ja031696+
(19) Kahn, M. L.; Monge, M.; Colliere, V.; Senocq, F.; Maisonnat, A.; Chaudret, B. "Size- and shape-control of crystalline zinc oxide nanoparticles: a new organometallic synthetic method", *Advanced Functional Materials* **2005**, *15*, 458, doi:
(20) Andelman, T.; Gong, Y.; Polking, M.; Yin, M.; Kuskovsky, I.; Neumark, G.; O'Brien, S. "Morphological Control and Photoluminescence of Zinc Oxide Nanocrystals", *J. Phys. Chem. B* **2005**, *109*, 14314, doi:
(21) Greene, L. E.; Yuhas, B. D.; Law, M.; Zitoun, D.; Yang, P. "Solution-Grown Zinc Oxide Nanowires", *Inorganic Chemistry* **2006**, *45*, 7535, doi:
(22) Luo, B.; Rossini, J. E.; Gladfelter, W. L. "Zinc Oxide Nanocrystals Stabilized by Alkylammonium Alkylcarbamates", *Langmuir* **2009**, *25*, 13133, doi: Doi 10.1021/La901830n
(23) Luo, B.; Kucera, B. E.; Gladfelter, W. L. "Synthesis and structures of zinc alkoxo, aryloxo and hydroxo complexes with an amidodiamine ligand", *Polyhedron* **2010**, *29*, 2795, doi:

(24) Huss, A. S.; Pappenfus, T.; Bohnsack, J.; Burand, M.; Mann, K. R.; Blank, D. A. "The Influence of Internal Charge Transfer on Nonradiative Decay in Substituted Terthiophenes", *J. Phys. Chem. A* **2009**, *113*, 10202, doi:
(25) Rossini, J. E.; Huss, A. S.; Bohnsack, J. N.; Blank, D. A.; Mann, K. R.; Gladfelter, W. L. "Binding and static quenching behavior of a terthiophene carboxylate on monodispersed zinc oxide nanocrystals", *J. Phys. Chem. C* **2011**, *115*, 11, doi:
(26) Huss, A. S.; Rossini, J. E.; Ceckanowicz, D. J.; Bohnsack, J. N.; Mann, K. R.; Gladfelter, W. L.; Blank, D. A. "Photoinitiated electron transfer dynamics of a terthiophene carboxylate on monodispersed zinc oxide nanocrystals", *J. Phys. Chem. C* **2011**, *115*, 2, doi:
(27) Huss, A. S.; Bierbaum, A.; Chitta, R.; Ceckanowicz, D. J.; Mann, K. R.; Gladfelter, W. L.; Blank, D. A. "Tuning Electron Transfer Rates via Systematic Shifts in the Acceptor State Density Using Size-Selected ZnO Colloids", *J. Am. Chem. Soc.* **2010**, *132*, 13963, doi:
(28) Bahnemann, D.; Kormann, C.; Hoffmann, M. In J. Phys. Chem. 1987; Vol. 91, p 3789.
(29) Spanhel, L.; Anderson, M. A. "Semiconductor Clusters in the Sol-Gel Process - Quantized Aggregation, Gelation, and Crystal-Growth in Concentrated Zno Colloids", *J. Am. Chem. Soc.* **1991**, *113*, 2826, doi:
(30) Schwartz, D. A.; Norberg, N. S.; Nguyen, Q. P.; Parker, J. M.; Gamelin, D. R. "Magnetic Quantum Dots: Synthesis, Spectroscopy, and Magnetism of Co2+- and Ni2+-Doped ZnO Nanocrystals", *J. Am. Chem. Soc.* **2003**, *125*, 13205, doi: 10.1021/ja036811v
(31) Xiong, W.; Laaser, J. E.; Paoprasert, P.; Franking, R. A.; Hamers, R. J.; Gopalan, P.; Zanni, M. T. "Transient 2D IR Spectroscopy of Charge Injection in Dye-Sensitized Nanocrystalline Thin Films", *J. Am. Chem. Soc.* **2009**, *131*, 18040, doi:
(32) Pellnor, M.; Myllyperkio, P.; Korppi-Tommola, J.; Yartsev, A.; Sundstrom, V. "Photoinduced interfacial electron injection in RuN3-TiO2 thin films: Resolving picosecond timescale injection from the triplet state of the protonated and deprotonated dyes", *Chem. Phys. Lett.* **2008**, *462*, 205, doi:
(33) Watson, D.; Meyer, G. "Electron injection at dye-sensitized semiconductor electrodes", *Annu. Rev. Phys. Chem.* **2005**, *56*, 119, doi:
(34) Anderson, N.; Lian, T. In Coord. Chem. Rev. 2004; Vol. 248, p 1231.
(35) Kallioinen, J.; Benko, G.; Myllyperkio, P.; Khriachtchev, L.; Skarman, B.; Wallenberg, R.; Tuomikoski, M.; Korppi-Tommola, J.; Sundstrom, V.; Yartsev, A. "Photoinduced ultrafast dynamics of Ru(dcbpy)(2)(NCS)(2)-sensitized nanocrystalline TiO2 films: The influence of sample preparation and experimental conditions", *J. Phys. Chem. B* **2004**, *108*, 6365, doi:
(36) Schwarzburg, K.; Ernstorfer, R.; Felber, S.; Willig, F. "Primary and final charge separation in the nano-structured dye-sensitized electrochemical solar cell", *Coord. Chem. Rev.* **2004**, *248*, 1259, doi:
(37) Murakoshi, K.; Yanagida, S.; Capel, M.; Castner, E. W. "Interfacial electron transfer dynamics of photosensitized zinc oxide nanoclusters", *Acs Sym Ser* **1997**, *679*, 221, doi:
(38) Trachibana, Y.; Haque, S.; Mercer, I.; Durrant, J.; Klug, D. "Electron injection and recombination in dye sensitized nanocrystalline titanium dioxide films: A comparison of ruthenium bipyridyl and porphyrin sensitizer dyes", *J. Phys. Chem. B* **2000**, *104*, 1198, doi:

(39) Kamat, P. V. "Photochemistry on nonreactive and reactive (semiconductor) surfaces", *Chemical Reviews (Washington, DC, United States)* **1993**, *93*, 267, doi:
(40) Demanze, F.; Cornil, J.; Garnier, F.; Horowitz, G.; Valat, P.; Yassar, A.; Lazzaroni, R.; Bredas, J. "Tuning of the electronic and optical properties of oligothiophenes via cyano substitution: A joint experimental and theoretical study", *J. Phys. Chem. B* **1997**, *101*, 4553, doi:
(41) Hapiot, P.; Demanze, F.; Yassar, A.; Garnier, F. "Molecular engineering of band level energies in oligothiophenes, through cyano-substitutions", *J. Phys. Chem.* **1996**, *100*, 8397, doi:
(42) Garcia, P.; Pernaut, J.; Hapiot, P.; Wintgens, V.; Valat, P.; Garnier, F.; Delabouglise, D. "Effect of End Substitution on Electrochemical and Optical Properties of Oligothiophenes", *J. Phys. Chem.* **1993**, *97*, 513, doi: